Prediction of draft force for Ard plows using dimensional analysis in silt loam soil

G. Thomas[1*], Y. Teshome[2], W. Amana[1]

(1. Adama Science and Technology University, Nazareth,P.O.box 1888, Ethiopia;

2. Wolkite University, Wolkite, P.O.box 03, Ethiopia)

Abstract: The proper amount of draft force required to till the soil is not coincide with the power applied in the field area during tillage of the soil. There is a need for investigation to predict the draft force of ard plow to improve our understanding of selecting appropriate input parameters for designing tools, which will help improve the allocation of the right prime power for a particular soil type. Otherwise, an excess load under load is applied and causes fatigue and inconvenience for both small-scale tools and operators. The aim of this research is to determine the draft force of Ard plough in silt loam soil. Laboratory and field tests were taken to measure actual draft force which was utilized as input for draft prediction. PI-Buckingham's pi theorem using dimensional analysis used to develop a mathematical model. IBM SPSS statistics software was applied to validate and verify the developed model. The relationship between the measured and predicted values of the draft force evaluated R^2 is 0.91. The predicted draft force value of skewness and kurtosis is in the range of accepted values. The performance of predicted draft force checked using RRMSE and CRM. Investigation findings demonstrate that derived mathematical equation was successful and viable for predicting the draft force of an ard plow in a silt loam soil.

Keywords: ard plow, dimensional analysis, draft force, mathematical equation, silt loam soil.

1 Introduction

Small-scale tillage tools are implemented on soil disturbances for seedbed preparation. The resistance force created by the soil and external force through tools used to move the soil is the key to the mechanics of soil-tool interaction. Several factors verify the required external force to disrupt the soil. It includes soil texture, properties of soil, geometries of tillage tools, and operating conditions of tillage. The prime mover of the draft force can be tractors (heavy having greater than 33.56 KW, medium having 18.64–33.56 KW, small having 11.18–18.64 KW), animal draught, or only human power. It is obvious that the tillage times spent on tillage vary according to the amount of power generated.

Many agree on achieving sustainable development goals of agriculture mechanization with a special focus on heavy or medium power tractors for plowing. But, agricultural mechanization coverage in Ethiopia is less than 1% plowing using (Berhane et al., 2017). However, Ethiopia launched a mechanization strategy and started the task officially in 2014 (Deribe and Jaleta, 2019) and the AU has promised to change the hand hoe to mechanization by 2025 (Takele and Selassie, 2018). Until now, no significant change has been made to shift smallholder farmers to mechanization. The reason for such cases is expected that almost 90% of smallholders produce cereal crops such as Teff. The ox plow was made well suited to Ethiopian farmers (Aune et al., 2020). They still use animal draught as a major source of plowing

without any scientific input (Ayichew et al., 2021), draught animals are interested in the traction of smallholders (Mota-Rojas et al., 2021).

But, technology used is inappropriate for agricultural situations and of poor quality, and also the technical understanding of the farmers is partial (Jiang et al., 2020). There is a lack of appropriate design and selection of tools for draught animals and tractors. There is no well-established animal draught tillage tool design criterion that is capable of predicting tillage tool behavior. Gaps exist in farmers' understanding of how the selection of appropriate animal draught to particular soil types with changes in operating conditions and tool geometry.

Improvement and valuation of tillage implementation performance and draft force requirements in tillage action have been focused on designing the tools that will be appropriate and minimum draft selection by farmers on the productivity of tillage processes. A continuing process of using efficient and effective animal-drawn tillage powers will be an option to increase the productivity of smallholder farmers. With proper handling of draught animals, well-maintained tillage tools and appropriate matching of tillage tools with the required draft force will play a fundamental role in increasing the benefit to productive performances. It can inspire food security by increasing agricultural production for smallholders.

There is a need for investigation to predict the draft force of ard plow to improve our understanding of selecting appropriate input parameters for designing tools, which will help improve the allocation of the right prime power for a particular soil type. Otherwise, an excess load under load is applied and causes fatigue and inconvenience for both small-scale tools and operators.

Variables such as operating conditions, tool geometer, and soil properties can affect the cutting of tillage tools. Selecting an effective amount of input data can reduce the draft force that will meaningfully increase tillage time and productivity, thus improving the economics of smallholders and ensuring food

stability. Ard plow has its own basic geometric shapes. This creates questions on the contribution of the draft force on parameters such as the operator side angle and plowshare-leather strip distance adjustment on the performance and design of the ard plow. Various laboratory and numerical experiments and analyses were performed to over check these two parameters as input data to predict the draft force of the ard plow in silt loam soil, which aided in selecting the appropriate input data. Empirical, analytical, and numerical methods are the most commonly used methods for analyzing the influence of parameters on the draft force (Abbaspour-Gilandeh et al., 2018; Hoseinian et al., 2022). Such methods require experimental data to construct an empirical investigation that will relate to prediction to adjust and certify models. Considering all parameters and determining the accurate equations at which the minimum draft force desires apply would require a great deal of study; mathematical modeling can provide a forecasting tool and the ability to modify variables. There have been numerous papers modeling predicting tillage tools; however, often they lack inclusive detailed parameters for the types of machinery operators walking behind them. Buckingham's pi theorem using dimensional analysis based on Microsoft Excel is needed since dimensional analysis approaches minimizing the number of input variables, and the IBM SPSS statistics package validates the draft force of tillage tools. Generally, the objective of this research is to generate mathematical model for prediction the draft force of ard plow in silt loam soil that will help for small scale farmers select appropriate draught animals.

2 Materials and methods

2.1 Description of site

The latitudes of Cheha Woreda, Ewan Kebele located 7.99 and 8.25 in the north and 37.59 and 38.06 in the east at a height of 1893 meters. Its average temperature varies from $18\,°$ to $27\,°$ (Figure 1). Teff is the main crop grown, and the average farmer has a holding area of 1 hectare. The data was started

taken from July 1, 2021- July 30, 2021, which was

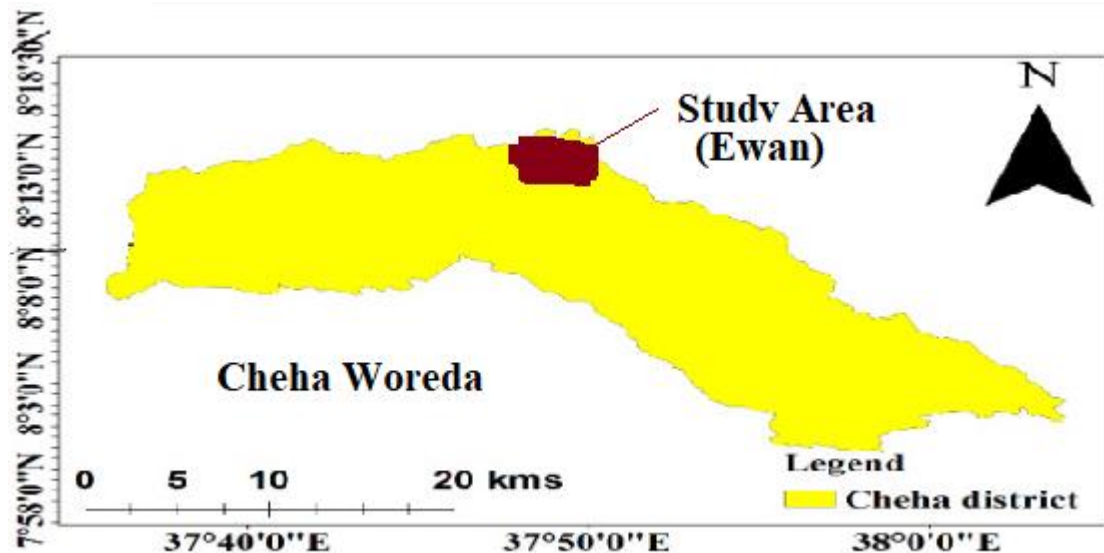after ten days of rainfall stated.

Figure 1 Map of Cheha woreda southern Ethiopia showing the study area

2.2 Soil properties

The percentages of clay silt and sand soil Table 1 was measured in field area and identified soil type using soil texture triangle. According to the texture triangle the soil texture found in the Ewan field area is silt loam.

Table 1 Percentage of soil texture in the field area

Sample	Percentage (%)
Clay	18.69
Silt	72.47
Sand	8.84

2.3 Field experimental procedure and design

2.3.1 Determination of soil moisture content

Twelve soil samples were gathered from both the dry and rainy field areas, totaling seven days of rain (wet). This testing procedure complies with ASTM standards for assessing soil moisture content in a laboratory. It focuses on the percentage representation of the weighted water content of soil material. This standard calls for drying the soil at a high temperature in an oven. The sample is mass-consistently dried in an oven.

$$M.C = \frac{WW-DW}{DW} \times 100 \qquad (1)$$

Where: M.C is moisture content, WW is weighted water content of soil material, DW is dried weighted content of soil material.

The following items are needed for this testing process (Figure 2):

An oven maintains a uniform temperature of all around the drying chamber. It keeps the drying chamber's interior at a constant temperature of 110 ℃±5 ℃ containers for sample drying and a balance with 0.01 g precision. Pinching hot gadgets is advised.

Figure 2 soil moisture laboratory test equipment

Dry samples should be prepared in a container, and then weighed on a balance. To grind up materials into a powder fine enough for a soil sample to pass through a 2.00 mm (#10) sieve, use a mortar or pestle

with a rubber covering.

1. In the sample container, note the sample's weight and code.

2. In the drying oven, dry the samples at 105 ℃

for 24 hours.

3. Before weighing the dried samples, remove the samples from the oven and allow them to cool to room temperature.

2.3.2 Determination of bulk density of soil

The bulk density test is one indication of the compaction rate of the soil. One method to determine the Bulk density of the soil is using core cutter as per standard code 2720529. Undistorted soil from the experiential field is taken.

The following material is used for taking samples

Figure 3 soil samples from field and soil mass

Testing Procedure:

1. Uncover a small area of the soil to be tested and flatten the surface, about 300 mm square in area.

2. Fix the dolly over the top of the core cutter, and press the core cutter into the soil mass using the rammer. Stop the pressing when about 15 mm of the dolly protrudes above the soil surface.

3. Remove the soil surrounding the core cutter, and take out the core cutter. The soil would project from the lower end of the cutter.

4. Remove the dolly. Trim the top and bottom surfaces of the core cutter carefully using a straight edge.

5. Weigh the core cutter filled with soil to the nearest gram (M_2).

6. Remove the core of the soil from the cutter. Take a representative sample to determine the moisture content.

7. Determine the water content.

Calculate:

The bulk density of the soil was calculated as follows:

$$\gamma_b = \frac{w_s - w_c}{v_c} \qquad (2)$$

Where: γ_b is bulk density (g cm^{-3}), w_c is weight of

from field and in the laboratory for testing process:

1. An oven maintaining a uniform temperature of 110 ℃ ±5 ℃ all around the drying chamber.

2. A balance with an accuracy of 0.01g.

3. Cylinder core cutter (100mm internal diameter and 130mm height).

4. Steel rammer (weight 9 kg).

5. Palette knife.

6. Straight edge steel rule.

7. Sample extruder.

8. Water content determination apparatus.

core cutter (g), w_s is weight of wet soil (g) and v_c volume of dry soil (cm^3).

2.3.3 Determination of soil internal friction angle (φ) and cohesion (*C*)

Getting shear strength is the goal. Parameters are angle of friction and cohesion.

Sample preparation: Works corporation collected soil samples from the field area and submitted them for Ethiopian design and oversight.

ASTM D3080 is a reference standard.

1. Shear box equipment, which consists of:

a) A sample of $60 \times 60 \times 20$ mm was examined in a shear box that was 60 mm square and 50 mm deep. The box was split into two half horizontally using the proper spacing screws.

b) A shear box storage unit.

c) Two sets of grid plates, one with perforations and the other set plain.

d) A pair of 6 mm thick porous stones.

e) A base plate that resides inside the shear box.

Test Procedure:

1. Use a sample trimmer to prepare at least three samples.

2. Insert the lower block after fixing the shear box's upper portion to the saturated container's lower

portion.

3. Carefully place the upper loading block in place after placing the sample in the shear box. Position the box correctly on the shearing machine.

4. Hang a standard load of 10 kg using the loading yoke mounted on the steel ball and loading block.

5. Apply shear force so that a very small load is applied and the loading knob just touches the top of the shear box.

6. Take out the fixing screws (pins) that were holding the upper and lower halves of the box together.

7. Lift the upper half of the box by moving the spacing screws such that it is slightly larger than the largest dirt particles in the sample.

8. Set the proving (load) ring dial to zero, apply the shear force, and shear the sample gradually and steadily until the sample fails at the maximum shear force.

9. Conduct the test again on the same samples while increasing the typical loads by 20, 30, 40 kg, etc.

10. Using the same scale, plot the failure envelope with the normal stress as the abscissa and the shear stress as the ordinate.

11. Measure the line's slope to obtain the ordinate's cohesion, (C), and the angle of internal friction.

Physical and mechanical properties of the soil tested and measured and allocated in Table 2.

Table 2 Soil properties found in field area

V (m s^{-1})	P (m)	λ (degree)	D (m)	P (g cm^{-3})	C (kg ms^{-2})	CI (Nm^{-2})	φ (deg)	M (%)	Ms (kg)	g (m s^{-2})
0.61	0.15	57	0.10	1.07	19.34	1.58	26.28	29.00	14	9.8
0.61	0.15	57	0.10	1.08	19.44	1.61	26.29	30.19	14	9.8
0.61	0.15	57	0.10	1.12	19.56	1.63	26.33	30.20	14	9.8
0.61	0.15	60	0.15	1.17	19.64	1.66	26.39	29.20	14	9.8
0.61	0.15	60	0.15	1.12	19.61	1.63	26.39	30.19	14	9.8
0.61	0.15	60	0.15	1.22	19.78	1.75	26.43	31.20	15	9.8
0.63	0.15	63	0.20	1.22	19.78	1.74	26.26	29.00	15	9.8
0.63	0.15	63	0.20	1.31	19.82	1.80	26.29	30.19	15	9.8
0.63	0.15	63	0.20	1.36	19.94	1.89	26.43	31.20	15	9.8
0.63	0.18	57	0.10	1.39	20.00	1.92	26.48	29.00	14	9.8
0.63	0.18	57	0.10	1.39	20.00	1.92	26.49	30.19	14	9.8
0.63	0.18	57	0.10	1.41	20.01	1.94	26.54	31.20	14	9.8
0.65	0.18	60	0.15	1.43	20.03	1.96	26.59	29.00	14	9.8
0.65	0.18	60	0.15	1.43	20.11	1.97	26.62	30.19	14	9.8
0.65	0.18	60	0.15	1.43	20.21	1.98	26.65	31.20	15	9.8
0.65	0.18	63	0.20	1.47	20.31	2.01	26.66	29.00	15	9.8
0.65	0.18	63	0.20	1.48	20.47	1.98	26.69	30.19	15	9.8
0.65	0.18	63	0.20	1.49	20.59	2.01	26.72	31.20	15	9.8

Where: CI is cone index , g is gravitational acceleration

2.3.4 Determination of soil penetration resistance

Soil penetration resistance is a measure of the strength of the soil. to measure the compaction rate of the soil. A cone penetrometer instrument was used to measure soil penetration resistance. The reading was taken at depths of 10, 15, and 20 cm. The soil penetration resistance force is calculated as the force obtained from the dial reading divided by the cone base area.

$$P_R = \frac{F}{A} \qquad (3)$$

Where: P_R is penetration resistance in N m^{-1}, F is applied force and A is cross sectional area.

2.4 Ard plow specification

Geometrical dimensions (Table 2) of ard plow are shown in Figure 4 with overall length of 50 cm, width of 30 cm and 1.5 cm thickness.
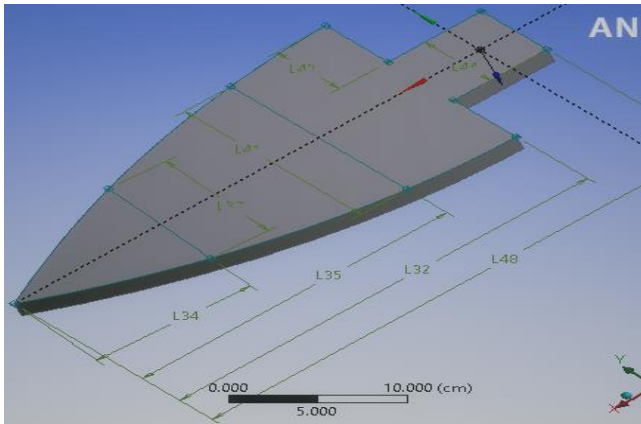

Figure 4 Ard plow geometry

Table 3 Specification of ard plow

Parts	L32	L34	L35	L48	L49	L50	L51
length (cm)	10	22	35	50	10	29	13

2.5 Experimental design

Three blocks, each measuring 60 m $\times$ 16 m, were developed for an experimental layout space measuring 60 m by 48 m. Each block was divided into 11 (eleven) strips, each measuring 60 m long by 1 m wide, with a 2 m gap between each strip.

Figure 5 Field layout

Zebu oxen are the main draft animals, weighing 250–300 kg, and they are largely used for seed-bed preparation (Gebregziabher et al., 2006) and they are taken as a source of power. The force data were measured using a spring balance capacity of 100 kg with an accuracy of 500 g. A hanging circular spring balance measured the pulling force of the tillage tool as it passed through the soil. It was converted to newton and multiplied by the cosine angle formed between the beam and the road surface as draft force.

Mixer (blender), hydrometer, sedimentation cylinder, control cylinder, thermometer, beaker and timing device were used to identify soil textures. A core cutter was used to determine the bulk density of undisturbed soil from the experiential field. An oven maintained a uniform temperature of 110 ℃±5 ℃ for the measured soil moisture content. Shear boxes were applied to measure soil cohesion (C) and internal friction angle (φ). A cone penetrometer instrument was used to determine the resistance forces of the soil.

2.6 Model development

2.6.1 Theory of dimensional analysis

Model calculating draft force (F_d) of ard plow in silt loam soil is based on creating of no dimensional groups. The parameters were arranged as unrepeated independent variables (Table 4).

Table 4 Dimensional matrix form of unrepeated variables

Dimension	F_d	CI	p	C	m_s	g
M	1	1	0	1	1	0
L	1	-1	1	-1	0	1
T	-2	-2	0	-2	0	-2

Table 5 Dimensional matrix form of repeated variables

Dimension	v	ρ	d
M	0	1	0
L	1	-3	1
T	-1	0	0

2.6.2 Formation of dimensionless groups

Dependent variable, independent variable and non-dimensional variables involved create dimensionless groups (Neela et al., 2013). It is constructed in the form of Equation 4.

$$\pi_1, \pi_2, \pi_3, \ldots \ldots \pi_{n-1}, \pi_n, \pi_{n+1} \tag{4}$$

An equation that divides unrepeated dimensions with repeated dimensions with a power of unidentified values was created to shift recurring and unrepeated dimensional variables into dimensionless groupings (Alghazali, 2012). This unknown number can be stated according to the matrix form of Equation 5.

$$[y] = [a]^{-1}[b] \tag{5}$$

The results of dimensionless groups and parameters without dimensions are listed below.

$$\pi_1 = \frac{F_d}{\rho v^2 d^2} \quad \pi_2 = \frac{p}{d} \quad \pi_3 = \frac{gd}{v^2} \quad \pi_4 = \frac{C}{\rho v^2} \quad \pi_5 = \frac{CI}{\rho v^2}, \quad \pi_6 =$$

$\frac{m_s}{\rho d^3}$, $\pi_7 = \varphi$, $\pi_8 =$, λ $\pi_9 = M$

Dimensionless groups were further combined to form reduced dimensionless groups through multiplication and division (Shafii et al., 1996).

A set of combined dimensionless parameters becomes.

$$\pi_{1,2} = f(\pi_{3,4}; \pi_{5,6}; \pi_{7,8}; \pi_9) \qquad (6)$$

Hence,

$$\frac{F_d}{\rho v^2 d^2} = f(\frac{\varphi}{1}, \frac{\lambda}{M}, \frac{gd\rho}{C}, \frac{CId^2}{v^2 m_s}) \qquad (7)$$

Meanwhile, the denominator of the dependent variables in Equation 8 is $\rho v^2 d^2$, the independent variable sides must be shifted and an outcome,

$$F_d = f(\frac{P\rho v^2 d}{\varphi}, \frac{P\rho v^2 d\lambda}{M}, \frac{Pgd^3 \rho^2 V^2}{C}, \frac{CId^3 P\rho}{m_s}) \qquad (8)$$

2.6.3 Determining fitness of input and validity of parameters for draft force prediction

Potential dimensionless arrangements have been evaluated using IBM SPSS statistical version 26 software by regression modeling and Microsoft Exel 2010. It was used to do a multivariate analysis of variance in order to determine the relationship between the predicted and experimental draft force results. By contrasting it with the experimental data, the created model's validity or suitability (goodness of fit) was evaluated. The constructed model's appropriateness was indicated by the establish R^2. Anything between 0% and 100% will do. It is the statistical indicator of how closely the data resemble the fitted regression line and referred to as the coefficient of determination. Higher R^2 values for the same data set indicate smaller discrepancies between the fitted values and the observed data. By dividing the regression sum of squares (SS_R) by the total sum of squares (SS_T), as per Equation 9 one can obtain the correlation coefficient (R^2).

$$R^2 = \frac{SS_R}{SS_T} \qquad (9)$$

However, if any combination has a lower correlation coefficient, it might not play a significant role in projecting draft force for the equivalent, therefore a the method of building regression models iteratively, which includes choosing independent variables to be included in the final model.

One of the methods most frequently used to assess the accuracy of forecasts when each residual is scaled against the actual value is using the relative root mean square error (Equation 10) and the coefficient of residual mass (CRM) which is persistence gauged by the residual mass-curve coefficient (Equation 8). If the discrepancies between the observed and predicted values are negligible and fair, a regression model fits the data effectively. The value of RRMSE must be less than 1 to good fit predicted model to the measure one. Otherwise, it simply indicating that model was unable to identify a suitable solution with optimization and having well performance (Thorp et al., 2007).

$$RRMSE = \sqrt{\frac{\frac{1}{n}\sum_{i=1}^{n}(y_i - \hat{y}_i)^2}{\sum_{i=1}^{n}(\hat{y}_i)^2}} \qquad (10)$$

Where n is the number of data points, y_i is the i-th measurement, and $\hat{y}_i$ is its corresponding prediction.

$$CRM = \frac{(\sum_{i=1}^{n} C_{measured} - \sum_{i=1}^{n} C_{predicted})}{\sum_{i=1}^{n} C_{measured}} \qquad (11)$$

A Z score is also a metric method which measure how closely a predicted value relates to the mean of a set of values for a verification check using the normality assumption. The Z score is quantified by the standard deviations from the mean. To ensure the confidentiality level, the measured draft force from the field area, the expected draft force from prediction and the forecasted draft force from prediction might all go through a normalcy check. We can use a numerical approach to verify this. Using skewness and kurtosis markers, the descriptive statistics clarified the secrecy level.

The formula for calculating skewness is given in Equation 12 and Equation 13.

$$Skewness = \frac{\sum(x - \bar{x})^3}{(n-1)*y^3} \qquad (12)$$

Where $\bar{x}$ the Mean and y is the standard deviation

$$kurtosis = \frac{\sum(x - \bar{x})^4}{(n-1)*y^4} \qquad (13)$$

Acceptable amounts of skewness range between $-$ 3 and $+$ 3, and kurtosis is suitable from a range of $-$ 10 to $+$ 10 when using SEM (Kenny and Editor, 2007).

3 Results and discussion

3.1 Model calibration

With recognized pertinent parameters, the non-dimensional consequence was identified Equation 4. The predicted numerical value for the expected draft forces of the group parameters x $(\frac{P\rho v^2 d}{\varphi})$, d $(\frac{P\rho v^2 d\lambda}{M})$, z $(\frac{Pgd^3\rho^2 V^2}{C})$ and Q $(\frac{CId^3 P\rho}{m_s})$ were displayed in Table 6.

Mathematical equations of each grouped parameters were listed in Equation 14, 15, 16 and 17.

The equations were constructed for each grouped parameters x, d, z, Q.

$$F_d \text{ measured } x = 6.98x + 274 \qquad (14)$$
$$F_d \text{ measured } d = 74.75\, d - 3.0 \qquad (15)$$
$$F_d \text{ measured } z = 31.86\, z + 2.4 \qquad (16)$$
$$F_d \text{ measured } = 0.16\, Q + 4.30 \qquad (17)$$

Table 6 the numerical value of x, d, z and Q

Predicted draft x	Predicted draft d	Predicted draft z	Predicted draft Q	Measured draft (N)
393.1	407.4	767.4	430.3	450.5
393.1	407.5	767.4	430.3	454.5
393.2	407.5	767.6	430.3	460.5
393.2	407.6	767.9	430.5	470.5
393.2	407.5	767.6	430.4	460.0
393.2	407.5	768.1	430.4	498.0
393.2	407.5	768.6	430.7	496.5
393.2	407.6	769.0	430.6	502.0
393.2	407.8	769.3	430.6	537.0
393.3	409.0	770.9	430.4	568.5
393.3	409.0	770.9	430.4	568.0
393.3	409.0	771.0	430.4	571.0
393.3	409.1	771.7	430.6	581.0
393.3	409.1	771.7	430.6	586.0
393.3	408.8	771.7	430.6	593.5
393.3	408.8	771.9	430.8	602.0
393.3	409.0	772.0	430.8	612.0
393.4	409.1	772.1	430.8	615.0

The achieved consequences exposed a significant outcome of the functions x, d, z and Q on the draft force presence considered. The calculation will have the notation of linear equation $y = ax + m$ and be used for arranging as addition or subtraction. Equations bounded by x, d, z and Q was created by combining each of the aforementioned-derived equations.

$$F_d = f_1(x, d, z, Q) + f_2(x, d, z, Q) + f_3(x, d, z, Q) + f_4(x, d, z, Q) \qquad (18)$$

Substitute grouped parameters which were highly correlated with draft force and became,

$$6.98(x) + 74.75\,(d) + 31.86\,(z) + 0.16\,(Q) - 277.7 = 0 \qquad (19)$$

Option -1

$$6.98(\tfrac{P\rho v^2 d}{\varphi}) + 74.75\left(\tfrac{P\rho v^2 d\lambda}{M}\right) + 31.86\,(\tfrac{Pgd^3\rho^2 V^2}{C}) + 0.16\left(\tfrac{CId^3 P\rho}{m_s}\right) = 277.7$$

Option -2

$$-6.98(\tfrac{P\rho v^2 d}{\varphi}) - 74.75\left(\tfrac{P\rho v^2 d\lambda}{M}\right) - 31.86\,(\tfrac{Pgd^3\rho^2 V^2}{C}) - 0.16\,(\tfrac{CId^3 P\rho}{m_s}) = -277.7$$

The real system must be evaluated over the range of quantities that the model will be used to predict to fully certify a model. The normalcy assumption must also be checked. The author calculated draft force equations that can be found in Equation 18 to anticipate the draft force of an ard plow. The

measured draft force values and predicted draft force value (Table 7). Verification and validation checks were carried out using IBM SPSS Statistical Software (Table 8).

Table 7 the value measured draft force values and predicted draft force value

Measured draft force from the field area (N)	predicted draft force taken from Equation option-1	predicted draft force taken from Equation option-2
450.50	413.40	18.44601
454.50	415.89	13.59296
460.50	417.92	10.12583
470.50	421.04	4.83984
460.00	418.06	9.986543
498.00	419.46	8.756684
496.50	419.69	9.469526
502.00	425.33	-0.16602
537.00	432.66	-13.9243
568.50	478.55	-101.875
568.00	478.55	-101.871
571.00	480.76	-105.855
581.00	484.38	-110.917
586.00	485.30	-112.823
593.50	473.54	-89.4323
602.00	477.17	-95.4567
612.00	484.41	-109.801
615.00	485.45	-111.683

3.2 Model validation

Evaluation of predicted and measured draft force concentration of ard plough tillage tools in silt loam soil is displayed in the Figure 6 (a b c d).
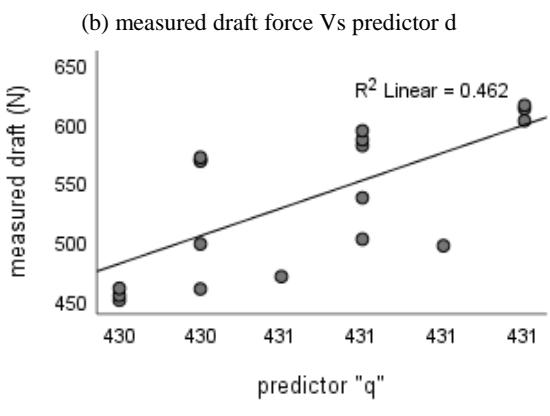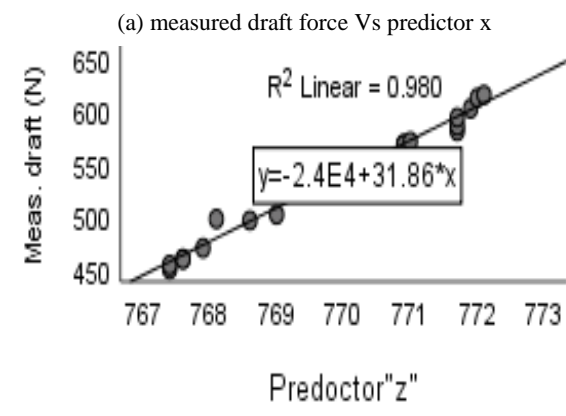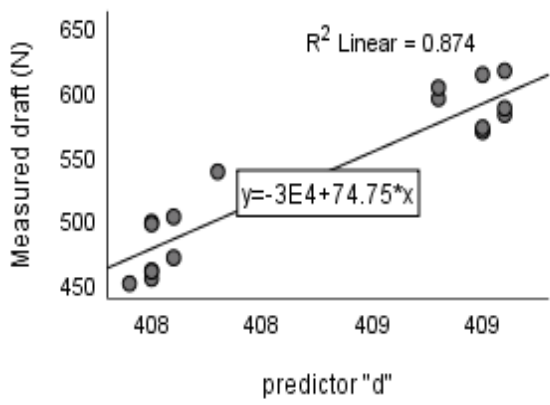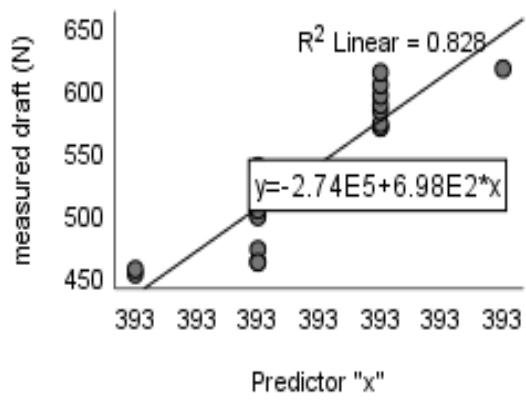
(a) measured draft force Vs predictor x

(b) measured draft force Vs predictor d

(c) measured draft force Vs predictor z

(d) measured draft force Vs predictor Q

Figure 6 Dependencies of non-dimensional groups' concentrations of x, d, z, Q

A Z score is a metric that measures how closely a value relates to the mean of a set of values for a verification check using the normality assumption of silt loam soil. The Z score is quantified by the standard deviations from the mean. To ensure the confidentiality level, the measured draft force from the field area, the expected draft force from Equation 15, and the forecasted draft force from Equation 19 might all go through a normalcy check. We can use a numerical approach to verify this. Using skewness and kurtosis markers, the descriptive statistics clarified the secrecy level.

Table 8 skewness and kurtosis values of predicted and measured draft force

	N	Mean	Std.	Skewness		Kurtosis	
	Stat	Statisti	Deviation	Statisti	Std. Erro	Statisti	Std. Error
Predicted draft 1	18	-48.8	57.8	.009	.536	-2.17	1.038
Measured draft	18	534.8	60.0	-.158	.536	-1.67	1.038
Predicted draft 2	18	450.6	31.5	-.019	.536	-2.15	1.038

The score standard of the measured draft and the expected draft force is normally distributed with a level of confidence of 99% given that both predicted draft forces are computed within the range of (-2.58, 2.58). The predicted value is having higher concentrations which, it indicate CRM less than zero (Slezingr and Purcz, 2013). The amount of RRMSE and CRM for both Predicted model are listed in Table 9.

Table 9 error for option-1 and option-2

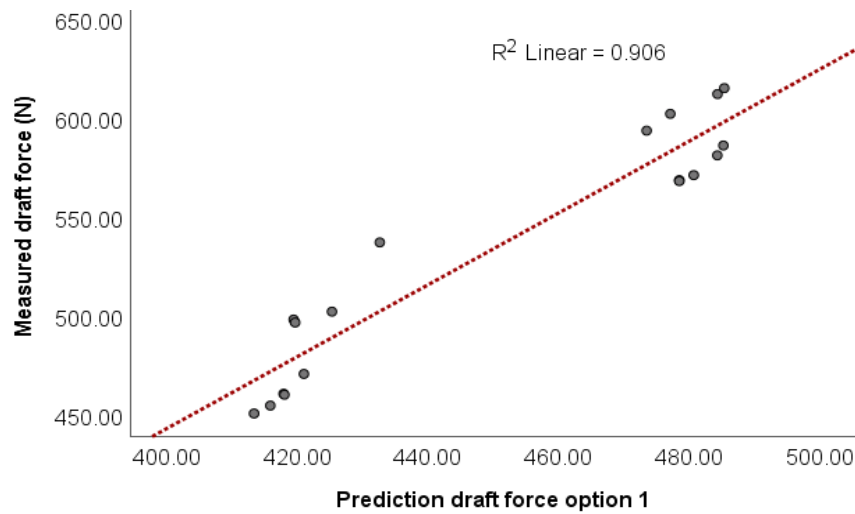| Pointer	Value of error for opt-1	Value of error for opti-2
RRMSE	0.093	0.246
CRM	0.842	-0.091

Figure 7 Relationship between the measured and predicted draft forces for the summation parameters (option-1)
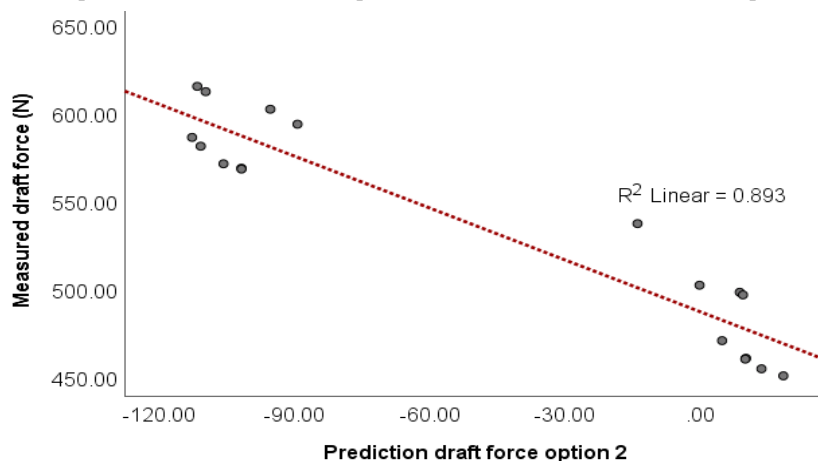

Figure 8 Relationship between the measured and predicted draft forces for the subtraction parameters (option-2).

3.3 Validity check of the model

Data found in the model that projected draft force for the tillage tool was made to stand up to scrutiny by connecting them with output data that were measured in an actual field area and assessed in the lab. Suitable statistical methods, general linear models, were applied to conduct validation checks. Before regression analysis yielded the coefficients of determination, the parameters that were entered as option-1 and option-2 to produce the predicted draft force data were plotted against the value of the measured draft results. The coefficients of determination for Figure 7 and Figure 8 are 0.906 and 0.893, respectively.

There is less significant difference between the amounts of measured and predicted values in both equations. However, option-2 has fewer coefficients of determination compared to option-1. Therefore, option-1 has better coefficients of determination and was developed as a mathematical model to predict the draft of ard plow on silt loam soil.

4 Conclusion

The current study has developed mathematical model of ard plow operating in silt loam soil proposed using PI-Buckingham's pi theorem in dimensional analysis. This model was examined and validated using IBM SPSS statistics software. The obtained data showed a strong correlation between the anticipated and measured draft forces ($R^2 = 0.906$), with no discernible difference between them. From the analytical presented, it is also within acceptable error range. This suggests that the equation is appropriate and acceptable for use in determining the ard plow's minimum draft force, which will reduce farmers' loss of power, direct them to choose the right prime power and be beneficial as input data for ard plow designers.

Conflict of Interest

The authors declare no conflict of interest. (Kenny, D. A. and S. Editor 2007).

References

Abbaspour-Gilandeh, Y., F. Hasankhani-Ghavam, G. Shahgoli, V. R. Shrabian, and M. Abbaspour-Gilandeh. 2018. Investigation of the effect of soil moisture content, contact surface material and soil texture on soil friction and soil adhesion coefficients. *Acta Technologica Agriculturae*, 21(2): 44–50.

Alghazali, N. O. S. 2012: A new method of dimensional analysis (Fluid mechanics applications). *Jordan Journal of Civil Engineering*, 6(3): 361–372.

Aune, J. B., M. T. Bussa, F. G. Asfaw, and A. A. Ayele. 2001.The ox ploughing system in Ethiopia: Can it be sustained? *Outlook on Agriculture*, 30(4): 275–280.

Berhane, G., M. Dereje, B. Minten, and S. Tamru. 2017. *The Rapid–But From A Low Base–Uptake of Agricultural Mechanizationin Ethiopia : Patterns, Implications and Challenges*. ESSP Working Paper 105. Washington, D.C. and Addis Ababa, Ethiopia: International Food Policy Research Institute (IFPRI) and Ethiopian Development Research Institute (EDRI).

Brown, Timothy A., 1960– Confirmatory factor analysis for applied research / Timothy A. Brown. — Second edition. (Methodology in the social sciences) Includes bibliographical references and index. ISBN 978-1-4625-1779-4.

Deribe, Y., and M. Jaleta. 2019. *Review of National Policies Influencing the Expansion of Agricultural Mechanization in Ethiopia. December 2019*. Mexico: International Maize and Wheat Improvement Center.

Gashu, M. W. 2022. Integration of Remote Sensing and Google Earth Engine for Land Use/Land Cover Change Analysis in Small Agricultural Watershed (A Case of Brante Watershed, Ethiopia). Available at: https://www.researchsquare.com/article/rs-2014415/v1.

Gebregziabher, S., A. M. Mouazen, H. Van Brussel, H. Ramon, J. Nyssen, H. Verplancke, M. Behailu, J. Deckers, and J. De Baerdemaeker. (2006). Animal drawn tillage, the Ethiopian ard plough, maresha: A review. *Soil and Tillage Research*, 89(2): 129–143.

Haile, G., F. Itanna, B. Teklu, and G. Agegnehu. 2022. Variation in soil properties under different land use types managed by smallholder farmers in central Ethiopia. *Sustainable Environment*, 8(1): 10–15

Hoseinian, S. H., A. Hemmat, A. Esehaghbeygi, G. Shahgoli, and A. Baghbanan. 2022. Development of a dual sideway-share subsurface tillage implement: Part 2. Effect of tool geometry on tillage forces and soil disturbance characteristics. *Soil and Tillage Research*, 215: 105200.

Jiang, X., J. Tong, Y. Ma, and J. Sun. 2020. Development and verification of a mathematical model for the specific resistance of a curved subsoiler *Biosystems Engineering*, 190(31970454): 107-119.

Mota-Rojas, D., A. Braghieri, A. Álvarez-Mac ás, F. Serrapica, E. Ram ŕez-Bribiesca, R. Cruz-Monterrosa, F. Masucci, P. Mora-Medina, and F. Napolitano. 2021. The use of draught animals in rural labour. *Animals*, 11(9): 2683.

Neela Deshpande, Shreenivas Londhe, Sushma Kulkarni. 2014. Modeling compressive strength of recycled aggregate concrete by Artificial Neural Network, Model Tree and Non-linear Regression, International Journal of Sustainable Built Environment,Volume 3, Issue 2,Pages 187-198. https://doi.org/ 10.1016/j.ijsbe.2014.12.002. (https://www.sciencedirect.com/science/article/pii/S221 2609014000569).

Shafii, S.K. Upadhyaya, R.E.1996. Garrett, The importance of experimental design to the development of empirical prediction equations, Trans. ASAE 39(2). 377e384.

Takele, A., and Y. G. Selassie. 2018. Socio-economic analysis of conditions for adoption of tractor hiring services among smallholder farmers, Northwestern Ethiopia of tractor hiring services among smallholder. *Cogent Food and Agriculture*, 4(1): 1–15.

Thorp, K. R., R. W. Malone, and D. B. Jaynes. 2007. Simulating long-term effects of nitrogen fertilizer application rates on corn yield and nitrogen dynamics. *Transactions of the ASABE*, 50(4): 1287–1303.

Workneh, W. A., Ujiie, K., & Matsushita, S. (2021). Farmers' agricultural tractor preferences in Ethiopia: a choice experiment approach. Discover Sustainability, 2(1). https://doi.org/10.1007/s43621-021-00021-2.

Zeleňáková, M., Čarnogurská, M., Šlezingr, M., Słyś, D., & Purcz, P. (2013). A model based on dimensional analysis for prediction of nitrogen and phosphorus concentrations at the river station Ižkovce, Slovakia. *Hydrology and Earth System Sciences*, 17(1), 201-209.